

# Sensing Weak Magnetic Fields By Living Systems and a Magnetoreception Mechanism For Navigation

Sergey Edward Lyshevski

Department of Electrical Engineering, Rochester Institute of Technology, Rochester, NY 14623-5603, USA  
E-mail: Sergey.Lyshevski@mail.rit.edu Web: www.rit.edu/~seleee

## ABSTRACT

The fundamentals for sensing weak magnetic fields in biological and *engineered* systems are researched. Our major goals are to study biophysics and apply cornerstone concepts examining existing premises and devising sound alternatives. The reported fundamental findings are applied. The feasibility analysis of proof-of-concept *solid* (silicon) and *hybrid* microdevices are documented.

**Keywords:** biosystems, magnetic field, sensing

## 1. INTRODUCTION

Some bacteria, migrating ants, bees, birds, fish, lobsters, salamanders, sea turtles and other living organisms likely exhibit the ability to sense the Earth's magnetic field and utilize the topographical mapping of the geomagnetic field for navigation, homing, foraging, etc. [1-17]. The magnetic properties of the closely-spaced biomineralized magnetite chains (~50 nm in diameter and length magnetites with ~5 nm separation) are utilized by magnetotactic bacteria for propulsion [3]. The iron oxide particles and their complexes are found in various living organisms, some of which are illustrated in Figure 1. These facts led to a hypothesis that intracellular biomineralized iron oxides could interact with the geomagnetic field thereby sensing its direction, variations, intensity and gradient. The cornerstone processes and mechanisms, utilized by living systems to detect the geomagnetic field, have being debated and are under extensive studies [1-17].



Figure 1. Fire ant, rainbow trout (*Oncorhynchus mykiss*), sockeye salmon (*Oncorhynchus nerka*) and homing pigeon

A great variety of biomineralized iron oxide particles (maghemite  $\gamma\text{-Fe}_2\text{O}_3$  and  $\varepsilon\text{-Fe}_2\text{O}_3$ , magnetite  $\text{Fe}_3\text{O}_4$ , hematite  $\alpha\text{-Fe}_2\text{O}_3$  and  $\beta\text{-Fe}_2\text{O}_3$ , wuestite  $\text{FeO}$  and other) were found within distinct orientation, patterns, etc. The size, shape, morphology, crystallography, spacing, magnetic moment orientation (single-domain, two-domain, superparamagnetic, etc.), magnetic dipole moment, magnetic and thermal stability, as well as other properties of biomineralized iron oxide particles and clusters vary.

The biomineralized magnetic iron oxides and corresponding receptors could constitute magnetoreceptor cellular assemblies within the peripheral and central nervous systems. Theoretically, these magnetoreceptors can sense the geomagnetic field utilizing the electrochemo-mechanical transitions. In addition, memory storage and retrieval can be accomplished.

## 2. FEASIBILITY ANALYSIS

The fundamentals of sensing, information retrieval, memory and processing by biosystems remain to be coherently researched performing fundamental and experimental studies. These findings may lead to alternative solutions and re-assessment of basic postulates and premises. The various aspects of magnetoreception (possible mechanisms, phenomena, effects, system organization, etc.) are important due to possible implications to *engineered* systems. We research:

1. Possible biophysics for sensing geomagnetic fields by biosystems, memory storage and memory retrieval;
2. Synthesis and design of *engineered* systems to sense magnetic fields.

Assuming the validity of the magnetic field sensing premise by biosystems, there are many fundamentally distinct phenomena, effects and mechanisms which potentially can be utilized. They range from the quantum mechanics (metastable states, quantization, spin-orbit interaction, etc.) to classical electromagnetics and microfluidics [18]. For example, an electron may have a spin magnetic dipole moment  $\mathbf{m}_{\text{spin}} \pm 9.27 \times 10^{-24} \text{ A}\cdot\text{m}^2$  with the alignment aiding or opposing an external magnetic field. As illustrated in Figure 2, there are small variations of the geomagnetic field which imply very small variations of the *microscopic* system energetics. Though these variations can be utilized by *microscopic* systems ensuring overall functionality and soundness, the resulting changes and transitions may or may not be observed and characterized due to fundamental and technological limits. In particular, the Heisenberg uncertainty principle provides the position-momentum and energy-time limits on the measurements as  $\sigma_x \sigma_p \geq \frac{1}{2}\hbar$  and  $\sigma_E \sigma_t \geq \frac{1}{2}\hbar$ .

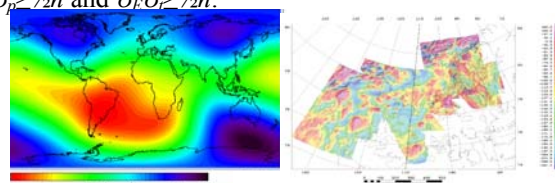


Figure 2. Variation in the Earth's magnetic field

Organic magnets may not exhibit sufficient changes to the mesoscale cellular structures at room temperature. For  $\alpha$ -1,3,5,7-tetramethyl-2,6-diazaadamantane-N,N'-doxyl,  $[\text{Fe}^{\text{III}}(\text{C}_5(\text{CH}_3)_5)_2]^+[\text{tetracyanoethylene}]^-$ , as well as  $\alpha$ - and  $\beta$ - $[\text{Fe}^{\text{III}}(\text{C}_5(\text{CH}_3)_5)_2]^+[\text{tetracyanoquinodimethane}]^-$  it was found that the Curie temperature is 1.48K, 4.8K, 2.55K and 3K, the saturation magnetization is 48300, 37600, 34200 and 21600 A/m, while the coersivity is very low.

For *microscopic* systems, the developments may be centered on individual molecules or their assemblies studying specific quantum effects, bond formation/braking, conformation and other phenomena which may be exhibited and utilized to ensure overall functionality at the device and

system levels. These premises may be based on unverifiable hypotheses, limiting these developments mainly to theoretical studies. These advancements although having an essential theoretical importance, may not be expected to be materialized as a feasible technology in near future. We focus on the conventional electromagnetics for meso- and macroscopic systems for which well-developed technologies (CMOS, micromachining, synthetic chemistry and other) exist.

To potentially contribute to the biophysics of *natural* systems and apply the results to *engineered* systems, we study the interactive electromagnetic-mechanical phenomena of clustered magnets (magnetic particles) with various molecular (*microscopic*), mesoscopic and macroscopic (*bulk*) receptors' and sensors' assemblies. It is found that weak magnetic field variations result in sufficient changes in the mesoscopic system states and quantities. These transitions can be utilized guarantying the overall functionality. The sensing mechanism can be based on the changes of physical quantities (variations of strain, charge, conformation, etc.) caused by the interaction of magnetic clusters, which have the magnetic dipole moment  $\mathbf{m}(\mathbf{r})$ , with the field  $\mathbf{B}$ .

### 3. ELECTROMAGNETICS AND ITS APPLICATION

The magnetic clusters cause electromagnetic interactions. The resulting forces may exert on biomolecular assemblies which can form biological receptors. Single-domain uniform-lattice magnetite ( $\text{Fe}_3\text{O}_4$ ) from 30 to 100 nm with the coercivity  $\sim 40$  mT are found in bacteria [3]. In the pigeon beak, the  $\sim 3$  nm magnetites are arranged in organized  $\sim 1$   $\mu\text{m}$ -diameter ferromagnetic or superparamagnetic clusters (assembly of ferrimagnetic or ferromagnetic particles in non-ferromagnetic matrix) within dendrites. In addition, the maghemite clusters occur around the vesicle (diameter  $\sim 5$   $\mu\text{m}$ ) as well as  $\sim 10$   $\mu\text{m}$ -long bundles of single crystalline uniform square platelets ( $\sim 1 \times 1 \times 0.1$   $\mu\text{m}$ ) within the dendrite in the ordered pattern [15]. A ferromagnetic magnetite (the orbital and spin magnetic dipole moments obey  $|m_{\text{spin}}| > |m_{\text{orb}}|$ ) exhibits a response to an external magnetic field. We consider:

1. Electromagnetic interactions of macroscopic ferromagnetic and superparamagnetic particles/clusters which lead to electromagnetic-mechanically induced transitions in biomolecular assemblies. Single-domain magnetite has been localized in the nervous system of various living organisms, and, correspondingly, may result in the subcellular level of sensory, memory and processing;
2. Microfluidics. The ordered, disordered and controlled dynamic and static behavior of particles (typical size is from  $\sim 10$  nm to  $\sim 10$   $\mu\text{m}$ ) can be utilized resulting in the possible electromagnetic field-induced viscoelastic, strain-caused and other transitions. The behavior of magnetite clusters can be examined and utilized in *engineered* systems. There are concerns that the arrangement and morphology of the magnetite in the dendrites, receptors and subcellular structures may not comply or be comprehended.

There is contradicting data in magnetic properties of the biomineralized and synthesized iron oxide particles and clusters. For example, the reported coercivity  $\sim 10$  mT and magnetic dipole moment  $\sim 1 \times 10^{-17}$  A $\cdot\text{m}^2$  for a  $\sim 1$   $\mu\text{m}$  magnetite cluster were questioned. Maghemite  $\gamma\text{-Fe}_2\text{O}_3$  has inherent cation vacancies  $V$  in the octahedral positions. From  $4\text{Fe}_2\text{O}_3 \rightarrow 3\{\text{Fe}^{3+}\text{O}(\text{Fe}_{5/3}^{3+}\text{V}_{1/3})\text{O}_3\}$  one concludes that

possible order-disorder at different sites are affected by the synthesis methods resulting in distinct characteristics. Various methods have been reported to synthesize iron oxide particles [19]. For example, ferrous chloride tetrahydrate  $\text{FeCl}_2 \cdot 4\text{H}_2\text{O}$  and ferric chloride hexahydrate  $\text{FeCl}_3 \cdot 6\text{H}_2\text{O}$  can be used. To neutralize the anionic charges on the particles surface, 1N hydrochloric acid HCl is used. The major steps are depicted as the reaction:  $\text{FeCl}_2 + \text{FeCl}_3 \rightarrow \text{Fe}_3\text{O}_4 \rightarrow \gamma\text{-Fe}_2\text{O}_3$ . In the first step, Fe(II)/Fe(III) with the molar ratio 1:2 are dissolved in water with sonication. The resulting solution is poured into alkali solution. Then, the precipitate is collected using a magnet, and the supernatant is removed from the precipitate by decantation. Deoxygenated water is added to wash the powder, and the solution is decanted after centrifugation. After washing the powder, 0.01M HCl solution is added to the precipitate to neutralize the anionic charges on the particles surface. The resulting magnetite  $\text{Fe}_3\text{O}_4$  is separated by applying an external magnetic field. The magnetite can be transformed into maghemite crystallites by oxidizing them at  $\sim 300^\circ\text{C}$  by aeration.

Two typical magnetization-applied field ( $M$ - $H$ ) curves (with and without hysteresis) for  $\sim 5$  nm maghemite  $\gamma\text{-Fe}_2\text{O}_3$  spherical particles, synthesized utilizing distinct procedures, are illustrated in Figure 3. The ferromagnetic ( $M$ - $H$  curves with hysteresis) and superparamagnetic (no hysteresis) are observed. One recalls that  $\mathbf{B} = \mu_0(\mathbf{H} + \mathbf{M})$ ,  $\mathbf{M} = \chi_m \mathbf{H}$ ,  $\mathbf{B} = \mu_0 \mu_r \mathbf{H}$ , where  $\chi_m$  is the magnetic susceptibility;  $\mu_r = 1 + \chi_m$ . For  $\text{FeO}_3$  the magnetic molar susceptibility  $\chi_m V_m$  is  $7.2 \times 10^9$   $\text{cm}^3/\text{mol}$ , where  $V_m$  is the molar volume. For the organic compounds ( $\text{C}_2\text{H}_2$ ,  $\text{C}_6\text{H}_6$ ,  $\text{C}_6\text{H}_{12}\text{O}_2$ ,  $\text{C}_{20}\text{H}_{12}$ , etc.), the diamagnetic molar susceptibility varies as  $\sim [2.5 \text{ } 20] \times 10^7$   $\text{cm}^3/\text{mol}$ .

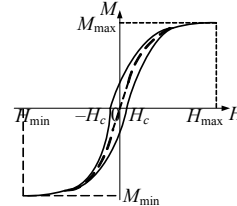


Figure 3.  $M$ - $H$  curves for  $\sim 5$  nm maghemite,  $H_{\text{max}}$  is  $\sim 100$  A/m

Consider the translational and *torsional-mechanical* motion of magnetic clusters in the magnetic field. The electromagnetic translational and rotational transitions result due to the force and torque developed. The torque  $\mathbf{T}$  tends to align  $\mathbf{m}$  with  $\mathbf{B}$ , and  $\mathbf{T} = \mathbf{m} \times \mathbf{B}$ . For a magnetic rod with the length  $l$  and the pole strength  $Q_m$ , the magnetic moment is  $m = Q_m l$ , while the force is  $F = Q_m B$ . The electromagnetic torque is  $T = 2F/2 \sin \alpha = Q_m l B \sin \alpha = m B \sin \alpha$ . Thus,  $\mathbf{T} = \mathbf{a}_m m \times \mathbf{B} = Q_m l \mathbf{a}_m \times \mathbf{B}$ , where  $\mathbf{a}_m$  is the unit vector in the magnetic moment direction.

With the average magnetic field of the Earth  $\sim 50$   $\mu\text{T}$ , which varies  $\sim \pm 0.5$   $\mu\text{T}$ , the torque is estimated to be  $\sim 1$  pN $\cdot\text{m}$ . The Newtonian translational and *torsional-mechanical* dynamics are governed by the differential equations  $\Sigma \mathbf{F} = m_m \mathbf{a}$  and  $\Sigma \mathbf{T} = J \boldsymbol{\alpha}$ . Here,  $\mathbf{a}$  and  $\boldsymbol{\alpha}$  are the linear and angular accelerations,  $\mathbf{a} = d\mathbf{v}/dt = d^2 \mathbf{r}/dt^2$  and  $\boldsymbol{\alpha} = d\boldsymbol{\omega}/dt = d^2 \mathbf{r}/dt^2$ ;  $m_m$  and  $J$  are the mass and moment of inertia.

Using the pole strength  $Q_m$ , the force acting on a magnet is  $\mathbf{F} = \mathbf{B} Q_m$ . The force between two magnets depends on the shape, magnetization, orientation, etc. The Coulomb law provides the equation for the force. For two magnetic

poles we have  $\mathbf{F} = \mathbf{a}_r \frac{\mu_0 Q_{m1} Q_{m2}}{4\pi r^2}$ , where  $\mathbf{a}_r$  is the unit vector along line joining poles;  $Q_{m1}$  and  $Q_{m2}$  are the pole strengths;  $r$  is the distance between poles. The flux density at distance  $r$  from a pole with  $Q_m$  is  $\mathbf{B} = \mathbf{a}_r \frac{\mu_0 Q_m}{4\pi r^2}$ .

The magnetization is defined as the *net* magnetic dipole moment per unit volume, e.g.,  $\mathbf{M} = \mathbf{m}/V = Q_m \mathbf{l}/V$ . For a uniformly magnetized cylindrical magnet of length  $l$  and cross-sectional area  $A$ , we have  $M = Q_m l / A l = Q_m / A$ . The pole surface density is  $\rho_{sm} = Q_m / A = M$ . For a cylindrical magnet with length  $l$  and radius  $r_m$ , the magnetic flux density on the axis is  $\mathbf{B} = \frac{1}{2} \mu_0 M \left( \frac{z}{\sqrt{z^2 + r_m^2}} - \frac{z-l}{\sqrt{(z-l)^2 + r_m^2}} \right) \mathbf{a}_z$ . The conformations

of the receptors (due to the exhibited electromagnetic force) are studied. The quantitative and qualitative analysis is performed to study the magneto-receptor-centered magnetic field sensing.

#### 4. INFORMATION STORAGE AND RETRIEVAL

Assuming the utilization of superparamagnetism, the energy required to change the direction of the particle magnetic moment is comparable to the ambient thermal energy. In ferromagnetic materials, the magnetic moments of neighboring atoms align, resulting in a large internal magnetic field. Superparamagnetism occurs when the temperature of material, composed of ~1 to 10 nm crystallites, below the Curie or Neel temperature (the thermal energy is not sufficient to overcome the coupling forces between neighboring atoms). Hence, the thermal energy is sufficient to change the direction of magnetization of the entire crystallite. Each atom is independently affected by an external magnetic field, and the magnetic moment of the entire crystallite tends to align with the magnetic field. Superparamagnetism establishes a limit on the minimum size of particles, resulting in constraints on the memory (storage) functionality, capabilities and density. The relative motion of the iron oxide particles/clusters with respect to each other can result in the longitudinal or perpendicular data storage (recording) which can be assessed and retrieved, see Figure 4. For the perpendicular storage, the memory density limit is ~1000 bit/ $\mu\text{m}^2$  which may be sufficient to ensure the geomagnetic field mapping by biosystems. The magnetization of the element should be retained despite thermal fluctuations caused by the superparamagnetic limit. The energy required to reverse the magnetization of a magnetic element is proportional to the size and the magnetic coercivity of the magnet. Biominerilized iron oxides could possess sufficiently large coercivity ensuring thermal stability thereby preventing demagnetization.

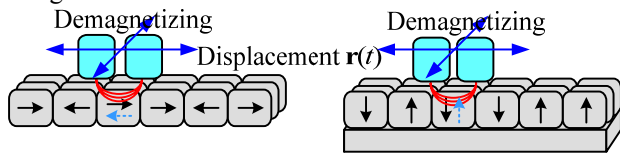


Figure 4. Longitudinal and perpendicular data storage utilizing electromagnetic- or pressure-induced magnetization: Demagnetizing and magnetic storage elements are in the relative motion

#### 5. ENGINEERED MAGNETIC FIELD SENSORS

Researching fundamentals of *engineered* magnetic field sensing devices, we concentrate on basic physics and current technologies to complement theoretical findings. The polymer chemistry and CMOS-centered technology are well-established ensuring high-yield mass-production. Maghemite, magnetite, hematite, wuestite and other oxides were synthesized and characterized. Polymer microcapsules with embedded magnetic particles can be synthesized. The polymer microcapsule's shells are formed as magnetic particles, dispersed in the hydrophobic polymer (for example, NOA prepolymer), are captured into the solid polymer phase at the emulsification step with the subsequent curing and drying. These oxides and microcapsules can be deposited on the movable diaphragm. The magnetic field can be sensed and measured as the membrane deflection or induced *emf*. The micromachined structures, components, proof-of-concept devices and *solid* (silicon) prototypes were designed and fabricated as reported in Figure 5.a [18, 20]. The deflection of the suspended (released) movable structures or diaphragms can be measured by using the variations of capacitance and resistance. For example, the micromachined four polysilicon resistors, which form the Wheatstone bridge, are documented in Figure 5.a [18, 20].

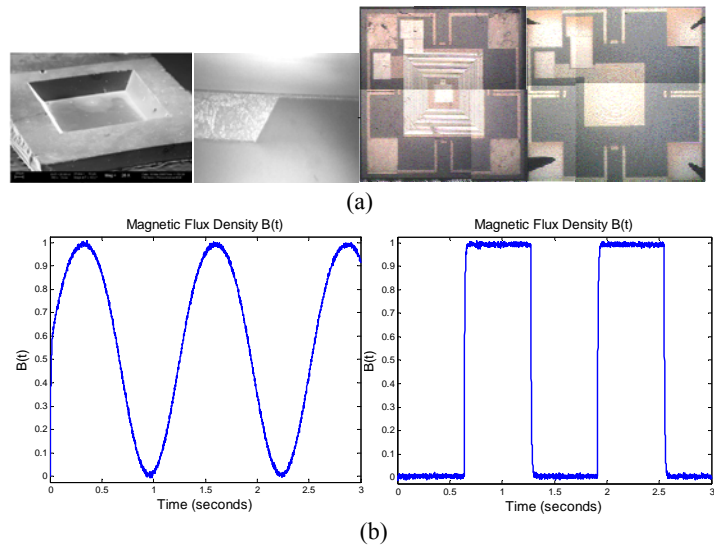


Figure 5. (a) Etched silicon structure, ~30  $\mu\text{m}$  silicon diaphragm, and micromachined sensors with polysilicon resistors (to measure the force-induced deflection) and Al coils on the silicon diaphragm; (b) Sensing time-varying  $B(t)$

The magnetic field is measured by using the force-induced displacement-centered sensing mechanism. Figure 5.b documents the deflection of the suspended diaphragm measuring  $B(t) = \frac{1}{2} [\sin(\frac{1}{4}\pi t) - 1]$  and  $B(t) = \frac{1}{2} [\text{rect}(\frac{1}{4}\pi t) - 1]$  mT. The noise  $\xi(t)$  can be filtered by ICs. We conclude that it is possible to accurately sense time-varying  $B$ . These sensors are key components of navigation systems.

In addition to *solid* concepts, *engineered fluidic* weak magnetic filed sensors are currently under development. We focus on soundness, technological feasibility, practicality

and device capabilities. Two possible solutions are briefly reported below.

Various magnetic particles can be coated by polymers and suspended in liquid and solid matrices. For example, the solvent-free surface-functionalized maghemite  $\gamma\text{-Fe}_2\text{O}_3$  can be functionalized by a positively-charged organosilane  $(\text{CH}_3\text{O})_3\text{Si}(\text{CH}_2)_3\text{N}^+(\text{CH}_3)(\text{C}_{10}\text{H}_{21})_2\text{Cl}^-$  which forms covalent bonds with the surface hydroxyl groups. A counter anion is  $\text{R}(\text{OCH}_2\text{CH}_2)_7\text{O}(\text{CH}_2)_3\text{SO}_3^-$ ,  $\text{R}:\text{C}_{13}\text{-C}_{15}$  alkyl chain. This ultimately may lead to an *engineered* inorganic apparatus to sense the magnetic field.

Protein complexes, which exhibit magnetic properties, can be synthesized [21-24]. For example, the ferritin protein, which consists of 24 protein subunits, is illustrated in Figure 6. Inside the ferritin shell, iron ions form crystallites with phosphate and hydroxide ions. The resulting complex is similar to the mineral ferrihydrite. Different physiological functionality of ferritin was defined. Ferritin can be used as a marker as well as a precursor. Native ferritin (iron-storage protein) has a spherical shell with an external diameter of 12 nm and an inner core diameter of 8 nm. A *natural* mammalian ferritin protein has an antiferromagnetic 8 nm iron oxyhydroxide core  $\text{Fe}(\text{O})\text{OH}$  with  $\sim 4500 \text{ Fe}^{3+}$  atoms. This core forms a noninteracting monodispersed superparamagnetic structure. Due to the structural defects and uncompensated surface moments, each iron oxyhydroxide particulate possesses a net magnetic moment due to uncompensated unpaired spins. The ferritin protein and other similar protein cages can be emptied of its contents and mineralized with different complexes [25-27]. With the embedded ferromagnetic maghemite  $\gamma\text{-Fe}_2\text{O}_3$ , the suspended *synthetic* ferritins can sense the magnetic field utilizing the force generation and displacement mechanisms.

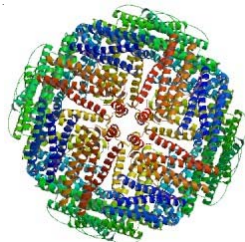


Figure 6. The crystallographic structure of the ferritin

## 6. CONCLUSIONS

Applying fundamentals of science and engineering, we outline and research established and potential paradigms in the sensing of weak magnetic fields. Our overall objective was to advance *engineered* solutions by developing alternative concepts observed in living systems. There is a need to span a wide range of multidisciplinary research activities focused on central issues of biophysics, neuroscience, engineering science and technology. This will lead to synergetic intellectual partnerships to strengthen the fundamentals of theoretical and applied science and engineering. We addressed important issues, studied *natural* systems, proposed possible inroads, and reported alternative solutions. These results promise a profound impact on the ability to create, generate and apply new knowledge contributing to scientific innovations in magnetic field sensing and navigation system designs.

## REFERENCES

1. T. Alerstam, *Bird Migration*, Cambridge University Press, Cambridge, 1990.
2. J. B. Anderson and R. K. Vander Meer, "Magnetic orientation in fire ant *Solenopsis invicta*," *Naturwissenschaften*, vol. 80, pp. 568-570, 1993.
3. R. P. Blakemore, "Magnetotactic bacteria," *Science*, vol. 19, pp. 377-379, 1975.
4. Y. Camlitepe and D. J. Stradling, "Wood ants orient to magnetic fields," *Proc. R. Soc. Lond. B*, vol. 261, pp. 37-41, 1995.
5. J. C. Diaz-Ricci and J. L. Kirschvink, "Magnetic domain state and coercivity predictions for biogenic greigite ( $\text{Fe}_3\text{S}_4$ ): A comparison of theory with magnetosome observations," *J. Geophys. Res.*, vol. 97, pp. 17039-17315, 1992.
6. C. E. Diebel, R. Proksch, C. R. Green, P. Neilson and M. M. Walker, "Magnetite defines a vertebrate magnetoreceptor," *Nature*, vol. 406, pp. 299-302, 2000.
7. D. M. S. Esquivel, D. Acosta-Avalos, L. J. El-Jaick, M. P. Linhares, A. D. M. Cunha, M. G. Malheiros and E. Wajnberg, "Evidence of magnetic material in the fire ants *Solenopsis* sp. by electron paramagnetic resonance experiments," *Naturwissenschaften*, vol. 86, pp. 30-32, 1999.
8. G. Fleissner, B. Stahl, P. Thalau, G. Falkenberg and G. Fleissner, "A novel concept of Fe-mineral-based magnetoreception: Histological and physicochemical data from the upper beak of homing pigeons," *Naturwissenschaften*, 2007.
9. J. L. Gould, "The case for magnetic sensitivity in birds and bees (such as it is)," *Am. Sci.*, vol. 68, pp. 256-267, 1980.
10. J. L. Kirschvink, "Magnetite biomineralization and geomagnetic sensitivity in higher animals: and update and recommendations for future study," *Bioelectromagnetics*, vol. 10, pp. 239-259, 1989.
11. J. L. Kirschvink, M. M. Walker, and C. E. Diebel, "Magnetite-based magnetoreception," *Current Opinion in Neurobiology*, vol. 11, pp. 462-467, 2001.
12. S. Mann, N. H. C. Sparks, M. M. Walker and J. L. Kirschvink, "Ultrastructure, morphology and organization of biogenic magnetite from sockeye salmon, *Oncorhynchus nerka*; implications for magnetoreception," *J. Exp. Biol.*, vol. 140, pp. 35-49, 1988.
13. T. P. Quinn, "Evidence for celestial and magnetic compass orientation in lake migrating sockeye salmon fry," *J. Comp. Physiol. A*, vol. 137, pp. 243-248, 1980.
14. H. Schiff and G. Canal, "The magnetic and electric fields induced by superparamagnetic magnetite in honeybees. Magnetoreception: an associative learning?" *Biol. Cybernetics*, vol. 69, pp. 7-17, 1993.
15. C. Walcott, "Magnetic orientation in homing pigeons," *IEEE Trans. Magnet. Mag.*, vol. 16, pp. 1008-1013, 1980.
16. R. Wiltschko and W. Wiltschko, *Magnetic Orientation in Animals*, Heidelberg: Springer-Verlag, Berlin, 1995.
17. S. Johnsen and K. J. Lohmann, "The physics and neurobiology of magnetoreception," *Nature*, vol. 6, pp. 703-712, 2005.
18. S. E. Lyshevski, *Molecular Electronics, Circuits, and Processing Platforms*, CRC Press, Boca Raton, FL, 2007.
19. R. G. C. Moore, S. D. Evans, T. Shen and C. E. C. Hodson, "Room-temperature single-electron tunnelling in surfactant stabilised iron oxide nanoparticles," *Physics E*, vol. 9, no. 2, pp. 253-261, 2001.
20. I. Puchades, R. Pearson, L. F. Fuller, S. Gottermeier and S. E. Lyshevski, "Design and fabrication of microactuators and sensors for MEMS," *Proc. IEEE Conf. Prospective Technologies and Methods in MEMS Design*, Polyana, Ukraine, pp. 38-44, 2007.
21. F. C. Meldrum, B. R. Heywood and S. Mann, "Magnetoferritin: in vitro synthesis of a novel magnetic protein," *Science*, vol. 257, pp. 522-523, 1992.
22. M. Okuda, K. Iwahori, I. Yamashita and H. Yoshimura, "Fabrication of nickel and chromium nanoparticles using the protein cage of apoferritin," *Bitech. Bioeng.*, vol. 84, pp. 355-358, 2003.
23. M. Okuda, Y. Kobayashi, K. Suzuki, K. Sonoda, T. Kondoh, A. Wagawa, A. Kondo and H. Yoshimura, "Self-organized inorganic nanoparticle arrays on protein lattices," *Nano Lett.*, vol. 5, pp. 991-993, 2005.
24. R. M. Kramer, C. Li, D. C. Carter, M. O. Stone and R. R. Naik, "Engineered protein cages for nanomaterial synthesis," *J. Am. Chem. Soc.*, vol. 126, pp. 13282-13286, 2004.
25. S. Gider, D. D. Awschalom, T. Douglas, K. Wong, S. Mann and G. Cain, "Classical and quantum magnetism in synthetic ferritin proteins," *J. Appl. Phys.*, vol. 79, pp. 5324-5328, 1996.
26. T. Douglas and M. Young, "Host-guest encapsulation of materials by assembled virus protein cages," *Nature*, vol. 393, pp. 152-155, 1998.
27. T. Douglas and V. T. Stark, "Nanophase cobalt oxyhydroxide mineral synthesized within the protein cage of ferritin," *Inorg. Chem.*, vol. 39, 1828-1830, 2000.